Laser pointing stabilization and control in the submicroradian regime with neural networks

F. Breitling,[a] R. S. Weigel, M. C. Downer, and T. Tajima[b]
Department of Physics, The University of Texas, Austin, Texas 78712

(Received 6 December 1999; accepted for publication 16 October 2000)

The possibility of controling the pointing stability of a slowly pulsed Ti:Sapphire laser system by lowpass filters and artificial neural networks (NN) is investigated by performing time series analysis and computer simulations on experimentally measured datasets. The simulations show that at pulse repetition rates of 20 Hz it is possible to use a feedforward algorithm to reduce the angular standard deviation from 0.7 to 0.3 μrad. The properties and advantages of NN methods such as automatic adaptation characteristics of a time series are discussed. © *2001 American Institute of Physics.* [DOI: 10.1063/1.1334624]

I. INTRODUCTION

Many laser applications, such as industrial processing, medical treatment, and atmospheric or orbital targeting in aeronautical, aerospace, or military fields require high laser power. To realize the high power, the laser energy is often accumulated and emitted in pulses. An important issue of these laser systems is the pointing stability. Since the position deviation of pulsed systems is only recorded when a pulse is emitted, the deviation of a later pulse cannot directly be corrected by opto-electronic feedback controllers that are designed for high repetition or continuous laser systems.[1–4] Instead, the deviation has to be estimated based on the preceding pulses. This extrapolating process is known as time series prediction, which can often be realized by filters[6] or often better by neural networks (NNs).[5–9]

In the following, it will be shown how to employ these methods for a particular high power laser system: a Ti:Sapphire laser system pulsed at 20 Hz, which is often used for laser acceleration experiments using wakefield.[10–12] The three major contributions to the pointing fluctuations are air convection in the beam path, mechanical vibrations of optical devices, and instabilities in the pump laser. Whereas the first two can be reduced further by changes in the experimental setup, the noise in the pump laser cannot and so determines the magnitude of the deviations to about 1 μrad. The goal is to find methods which can reduce this remaining standard deviation further. The theoretical limit of earlier implemented lowpass filters (LPFs)[13] as well as the possibility of new approaches using NNs will be discussed and their results will be determined based on computer simulations which use experimental data.

II. EXPERIMENTAL SETUP

A sketch of the experimental setup is shown in Fig. 1. The cavity of the regenerative Ti:Sapphire laser amplifier is pumped by a *Q*-switched Nd:YAG laser with a repetition frequency of 20 Hz. The out-coupled megawatt pulses pass eight mirrors before hitting a four-quadrant photodiode detector at a distance of 6 m.

The quadrants of the detector are connected to a sample and hold circuit. The induced current in each quadrant, which is proportional to the illuminated area by a pulse, is converted into a proportional voltage between 0 and 5 V and recorded by a computer. The x and y positions can be determined from the voltage (a,b,c, and d) of each quadrant (Fig. 1) by the linear approximations $x=(b+c-d-a)/(a+b+c+d)$ and $y=(a+b-c-d)/(a+b+c+d)$. This is a good approximation since the diameter of the pulses (2 mm) are about 1000 times larger than the measured deviations of a few μm at the detector. For a radial symmetric Gaussian profile, the relative error of a 2 μm shift due to nonlinear changes in the illuminated quadrants will be less than 10^{-4} as can be derived from geometrical considerations. The single pulse position resolution, determined by comparison with a second detector, is 0.25 μm which is equal to an angular resolution of 0.042 μrad. Hence, the error due to nonlinear changes in the illuminated quadrants is negligible.

III. TIME SERIES ANALYSIS

The following discussion of techniques of time series analysis are useful to gain insights into the predictability of time series and how to determine the appropriate method of the prediction.[14] The time series of the Ti:Sapphire laser system will be represented in x and y components. Although the beam wander in the y direction is about twice as strong as in the x direction, there is no significant difference between the two components in all other discussed aspects. Furthermore, no correlation between the two components, which would improve a prediction based on both components, is found. This was verified computationally since there was no prediction improvement on a network which used joint versus separate components. For this reason, the analysis is presented on only one component. The data sets contain 10 000 succeeding pulses recorded at the 20 Hz pulse repetition rate

[a]Electronic mail: fkbreitl@ph.utexas.edu
[b]Also at Lawrence Livermore National Laboratory, Livermore, California 94551.

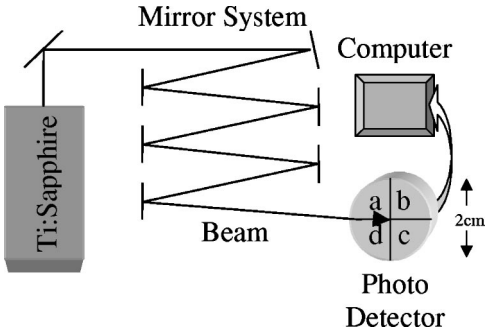

FIG. 1. Experimental setup for the detection of the position deviation of the pulses emitted from a Ti:Sapphire laser system with a four-quadrant photodiode detector and the recording by a computer.

over 8 1/3 min. A sample section of the time series which shows the beam wander in the x–y plane is shown in Figs. 2 and 3.

A. Power spectrum

The power spectrum is an important tool for determining the composition of periodic contributions to the position deviation below the 10 Hz Nyquist frequency. The power spectrum in Fig. 4 is obtained by the Welch's average method,[15] which gives a smoothed power spectrum by dividing the data into nonoverlapping subsections. Contributions at frequencies below 0.5 Hz are very significant. This shows that the major deviations originate from slow beam drifts. Slow beam drifts indicate that a LPF will provide a good correction. At higher frequencies, no significant periodic contributions are found and therefore further correction will be difficult, since the deviations that cannot be corrected by the LPF have only a small contribution.

B. Autocorrelation function

To find periodicities and estimate the effective dimension of the dynamical system which produces a time series, the autocorrelation function can be used:

$$c(\tau)=\frac{\langle (y_t-\overline{y})(y_{t+\tau}-\overline{y})\rangle}{\langle (y_t-\overline{y})^2\rangle}, \tag{1}$$

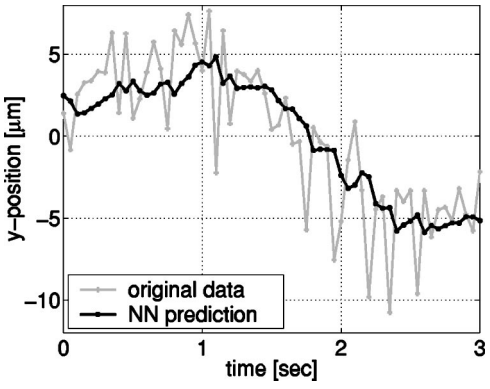

FIG. 2. Sample section of the time series showing typical beam wander. The y component of the radial pulse deviations at the detector are plotted vs time. For comparison, the deviation predicted by a NN is also shown. The LPF prediction is similar and omitted for clarity.

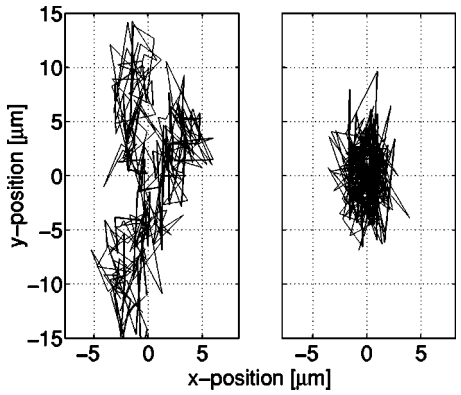

FIG. 3. Sample section of typical beam wander in the x–y plane. The deviations of the laser pulses in y direction are plotted vs the deviations in x direction. The uncontrolled system has an average radial standard deviation $\sigma=4.3$ μm (left-hand side panel), the same system with simulated controling by NN has a reduced average radial standard deviation $\sigma=2.0$ μm. The amplitude is determined as the difference between the predictions of a NN computer simulation and the actual deviation (right-hand side panel).

where N is the number of samples, y_t is the sample at time t, and τ is the time lag. Equation (1) reflects the mean correlation between each element of the time series and its τ-next neighbor. If $c(\tau)$ reaches an amplitude significantly different from zero after a few zero crossings, then the underlying process possesses a short term predictability. On our data, the autocorrelation function of the Ti:Sapphire series does not reveal any additional information besides that due to the dominant low frequency components.

C. Dimensional analysis

Based on the previous results, we additionally want to consider a dimensional analysis of the data which can be used to determine not only chaotic behavior but also the optimal size of the time delayed input vectors to be used for the prediction using a NN. For a chaotic system, the difficulties of prediction increase with the effective number of degrees of freedom, which can be measured by the dimensionality of the embedding. The number of inputs presented to the predicting system should be at least equal to the embed-

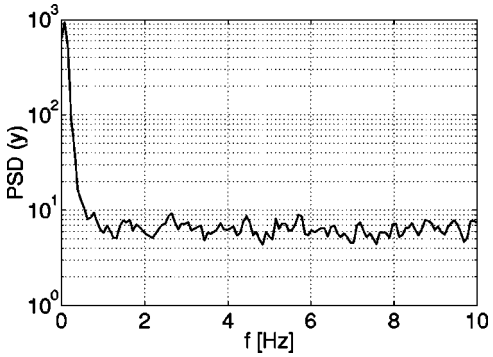

FIG. 4. Power spectrum of the time series of the y deviation of the pulses sampled at the pulse repetition rate of 20 Hz. Significant is the contribution at frequencies below 0.5 Hz representing a dominant slow beam wander.

ding dimension so that it contains the necessary information for a correct prediction. The embedding dimension is determined by the correlation integral

$$C(r)=\frac{1}{N(N-1)}\sum_{i,j=1}^{N}\Theta(r-|\vec{y}_i-\vec{y}_j|), \tag{2}$$

where N is the data set size, $\Theta(x)=0$, for $x<0$ and $\Theta(x)=1$, for $x\geqslant 0$.[16–18] Applying this method to the laser series does not provide the optimal input vector size, since a dimension above ten is found. Since the amount of data required to accurately determine embedding dimensions scales as A^D where D is the embedding dimension and $A>2$, there is a tremendous demand for data and the required computational effort is prohibitive.[19] Hence the optimal input vector size will be determined by trial and error by testing input vectors of various lengths and choosing the minimum length above which the predictive performance does not improve further.

IV. RELATION BETWEEN LPF AND NN

A lowpass filter is mathematically described by $\alpha(dy_t^{\text{out}}/dt)=y_t-y_t^{\text{out}}$ where y_t is the input, y_t^{out} is the output signal, and α is a time constant. If this equation if discretized, it is found that

$$y_{t+1}^{\text{out}}=\sum_{j=1}^{t} w_j y_j, \tag{3}$$

where the weights (w_t) are functions of α and the sample frequency. Equation (3) describes already a primitive neural network.

The difference between a NN and a LPF is that the NN has more freedom for choosing weights, allows a nonlinear input–output response through an activation function (g) and allows more freedom in the choice of input variables. Hence, a neural network can be more accurate in mapping input vectors to output vectors. Therefore, it is used in time series prediction for mapping time delayed input vectors ($\vec{y}_t$) onto their next values (y_{t+1}). Using $\vec{y}_t$ as an input, the form of a three layered feed-forward network, also known as multilayer perceptron, that was used for the predictions is given by

$$y_{t+1}^{\text{out}}=\sum_{j=1}^{M} w_j^{(b)} g\left(\sum_{i=t-\tau}^{t} w_{ji}^{(a)} y_i\right), \tag{4}$$

where g is the activation function, w are weights in the layers a and b, M is the number of units in the hidden layer, and τ is the input vector size. In the training process, the weights are adapted so that the actual value matches the predicted as well as possible. Mathematically this is expressed by minimizing the error function

$$E=\frac{1}{N}\sum_{t=1}^{N}(y_t^{\text{out}}-y_t)^2, \tag{5}$$

where N is the data set size. In practice, the data is split into a training and a validation set to ensure a good generalization.[20]

TABLE I. Standard deviation of the x and y components before and after different simulations of controling. The dominance of slow beam wander already allows a good improvement by a delay line. Improved results are obtained by the optimized LPF and a feed-forward NN which can reduce the overall deviation by more than 50%.

Data	σ_x (μrad)	σ_y (μrad)
uncontrolled	0.577	0.880
delay line	0.308	0.588
LPF	0.247	0.467
NN	0.245	0.463

V. PREDICTION AND RESULTS

Because of its simplicity, the delay line is briefly mentioned. It already gives surprisingly good predictions due to the dominant low frequency beam wander. A delay line simply predicts the next pulse deviation to be equal to the current. This is already a simple LPF. To simulate controling, the predicted deviation is subtracted from the actual one. Hence, for the delay line, the previous deviation is subtracted from the current which reduces the radial standard deviation by about one third (Table I).

Better results are obtained by controling through a LPF which is adapted to the time series. Only first order Butterworth LPFs are considered. To find the optimal LPF, the standard deviations for various cut-off frequencies are determined for the same data set. The optimal cut-off frequency is found at 0.09 Hz, where the simulated controling by the LPF prediction reduces the standard deviation of the time series by more than 50%; in the x direction (σ_x) from 0.577 to 0.247 μrad and in the y direction (σ_y) from 0.880 to 0.467 μrad (Table I).

Controling by NNs is simulated by feed-forward, elman, and cascade-forward NNs. They can be constructed by the neural network toolbox of the MATLAB software package.[21] Powell–Beale and Levenberg–Marquardt back propagation training algorithms as well as hyperbolic tangent sigmoid and linear transfer functions are used in various combinations. The network structure varies from (3-4-1) to (20-20-1) and even four-layered networks (a-b-2-1) are examined. The notation (a-b_1-b_2--c) stands for a units in the input layer, b_1 in the first hidden, b_2 in the second hidden, ..., and c units in the output layer. The input vector size is varied from 3–15 elements and the time lag τ was chosen for up to 50 samples. The results are not very sensitive to the network type or to these parameters. The best performance is achieved by the feed-forward network (4-5-1) trained using the Powell–Beale algorithm, sigmoid transfer functions in the first layer, linear transfer functions in the second layer, and time delayed vectors of $\vec{y}=(y_1,y_2,y_3,y_4)$ corresponding to the latest four samples. The correction by this method reduces σ_x to 0.245 μrad and σ_y to 0.463 μrad (Figs. 3, 4, and Table I).

We have shown that the angular deviation of this pulsed laser system can be reduced by more than 50% using either a LPF or NN. A comparison between the two methods shows a slightly improved but similar controling by NNs. This is not

surprising due to the dominance of slow beam wander. Since the NNs find predictable components automatically, their application is attractive where the power spectrum is more complex, no prior spectral characteristics are established, or where they are bound to change. The experimental implementation of the NN is straightforward. The theoretical corrections determined here for the NNs can be directly applied to a controller if the controling is applied on a separate mirror which is later in the beam path (after the position detector). This will prevent direct feedback from changes due to controling. A second detector might be required to calibrate or supervise the controling. On the other hand, NNs do not always provide significant prediction performance improvements, and hence do not generally justify the additional computational effort required for their realization. The examined Ti:Sapphire series is an example where dominant low frequencies conceal the superior adoption and prediction abilities of the NNs. The application of NNs to pulsed laser systems can be useful, and the success of NNs in nonlinear forecasting encourages our hopes towards a feed-forward controlled laser wakefield accelerator, since linear accelerators cannot be controlled by feedback.

ACKNOWLEDGMENTS

The work was supported by the DOE and the JAERI.

[1] S. Grafström, U. Harbarth, J. Kowalski, R. Neumann, and S. Noethe, Opt. Commun. **65**, 121 (1988).
[2] R. Heyler and S. C. Guggenheimer, Laser Focus World **27**, 107 (1991).
[3] E. W. Gaul, M.A. thesis, The University of Texas at Austin, 1993.
[4] C. W. Siders, E. W. Gaul, and M. C. Downer, Rev. Sci. Instrum. **65**, 3140 (1994).
[5] A. Weigend and N. Gershenfeld, *Proceedings of the NATO Advanced Research Workshop on Comparative Time Series Analysis* (Addison–Wesley, Reading, MA, 1994).
[6] J. V. Hernandez, A. Vannucci, and T. Tajima, Nucl. Fusion **36**, 1009 (1996).
[7] J. V. Hernandez, A. Vannucci, and T. Tajima, Nucl. Fusion **39**, 255 (1999).
[8] J. V. Hernandez, T. Tajima, and W. Horton, Geophys. Res. Lett. **20**, 2707 (1993).
[9] R. S. Weigel, W. Horton, T. Tajima, and T. Detman, Geophys. Res. Lett. **26**, 1353 (1999).
[10] T. Tajima and J. M. Dawson, Phys. Rev. Lett. **43**, 267 (1979).
[11] T. Tajima, S. Cheshkov, W. Horton, and K. Yokoya, AIP Conf. Proc. **8**, 153 (1999).
[12] T. Tajima, S. Cheshkov, W. Horton, and K. Yokoya, AIP Conf. Proc. **8**, 343 (1999).
[13] M. G. Goldammer, M. A. thesis, The University of Texas at Austin, 1996.
[14] F. Breitling, M. A. thesis, The University of Texas at Austin, 1999.
[15] *User's Guide: Signal Processing Toolbox*, The MathWorks, Inc., revised for MATLAB 5.2 (1998).
[16] P. Grassberger and I. Procaccia, Phys. Rev. Lett. **50**, 346 (1982).
[17] H. D. I. Abarbanel, Rev. Mod. Phys. **65**, 1331 (1993).
[18] Y. Kishimoto, J. K. Koga, T. Tajima, and D. L. Fisher, Phys. Rev. E **55**, 5948 (1997).
[19] A. Jedynak, M. Bach, and J. Timmer, Phys. Rev. E **50**, 1770 (1994).
[20] S. Haykin, *Neural Networks: A Comprehensive Foundation* (Prentice Hall, Upper Saddle River, NJ, 1999).
[21] *User's Guide, Version 3.0: Neural Network Toolbox*, The MathWorks, Inc. (1997).